CYBER-PHYSICAL MAGNETIC FIELD SENSORS

Vladimir Kravljaca and Sergey Edward Lyshevski
Department of Electrical and Microelectronic Engineering
Rochester Institute of Technology
Rochester, NY 14623, USA
E-mail: seleee@rit.edu; URL: http://people.rit.edu/seleee

ABSTRACT

This paper studies integrated solid-state Hall effect sensors with processing microelectronics. Many commercialized triaxial magnetometers have III-V semiconductor sensing elements, application-specific integrated circuits (ASICs) and microcontrollers. Processing algorithms are supported by device- and hardware specific architectures, middleware and software. Integrated Hall effect sensors with InSb sensing elements may ensure sufficient accuracy, measurement range, adequate spatiotemporal resolution, linearity, high bandwidth, and fast response time. Nonlinearities, cross-axis coupling, temperature sensitivity and other performance-degrading phenomena are minimized using ASICs which implement filters, compensators, etc. We examine and solve noise attenuation and error reduction problems by processing the ASICs outputs of integrated Hall effect sensors. Noise and error are minimized by using adaptive filters and information analysis. A dynamic mode estimator supports system reconfiguration. The experimentally substantiated laboratory-proven schemes enhance the existing solutions toward CPS-compliant sensing solutions for complex systems.

***Keywords*:** cyber-physical systems, Hall effect, magnetic field sensors, signal processing

1. INTRODUCTION

Cyber-physical systems (CPS) comprise compliant cyber-physical components with middleware and software. Big data information management, *cloud* computing, data fusion and processing algorithms are envisioned to be implemented. The CPS and Internet of Things (IoT) imply millions of interconnected devices to perform sensing, interaction and control in various applications. The current CPS technology cannot manage system complexity and heterogeneity under uncertainties in rapidly changing and adverse open environments. There is a need to foster design of autonomous peripheral CPS-compliant components by applying consistent science, concurrent engineering and transformative technologies. New methods, tools, hardware and software must be developed based upon the cross-cutting principles and their validation. Conventional sensing solutions are inadequate for large-scale, spatiotemporal and hierarchically-distributed CPS. Enhanced functionality smart sensors enable safety, reliability, redundancy, modularity, interface, interoperability, scalability and robustness.

Design of peripheral CPS-compliant components, including hierarchically centralized or decentralized integrated sensors, is the frontier in the technology developments. These sensors may enable information procurements, data analytics and knowledge generation at the source of the data. This approach empowers cognitive processing at the node level within the networked system organization. Using cooperative distributed sensors, one may accomplish peripheral *cloud* computing, distributed data storage and data retrieval. We consider integrated solid-state and MEMS sensors with ASICs and microcontrollers to implement processing at the nodes, thereby ensuring integration of computational algorithms and physical components. We research InSb Hall effect sensors to measure the spatiotemporal magnetic fields $\mathbf{B}(t,\mathbf{r})$, and, estimate field gradients $\nabla\mathbf{B}$ and graphs $f(\Sigma_i\mathbf{B})$. Commercialized one-, two- and three-axis Hall effect sensors are fabricated by Allegro MicroSystems, Honeywell, Melexis, Texas Instruments and other companies. Numerous challenges and problems exist [1-5]. Multispectral noise attenuation and error minimization problems are examined and solved to ensure the accuracy and spatiotemporal resolution of $\mathbf{B}(t,\mathbf{r})$, $\nabla\mathbf{B}$ and $f(\Sigma_i\mathbf{B})$. This will enable physical and processing data accuracy ensuring data conformity, consistency, completeness and validity. The post-processing on $\mathbf{B}(t,\mathbf{r})$ is examined using additional ASICs which implements adaptive filtering and estimation. The application of FPGA is studied.

2. DETECTION AND PROCESSING

Magnetic field sensors are used in aerospace, automotive, naval, energy, electronic, robotic, medical, security and other systems. Sensing $\mathbf{B}(t,\mathbf{r})$, $\nabla\mathbf{B}$ and $f(\Sigma_i\mathbf{B})$ advances persistent surveillance, reconnaissance, detection and tracking of *smart* targets. Accuracy, precision and sensitivity are of a particular importance in navigation systems, magnetic compasses, dead reckoning, displacement sensing, etc. We study the physical and processing limits in order to empower existing solutions to detect, measure, fuse and process spatiotemporal $\mathbf{B}(t,\mathbf{r})$. Migrating ants, bees, birds, fish, lobsters, salamanders, sea turtles and other living organisms exhibit the ability to sense the Earth's magnetic field and use topographical maps of the geomagnetic field for navigation, homing, foraging, etc. Magnetoreception, exhibited by bacteria, arthropods, molluscs and other organisms, implies the ability to sense magnetic fields in the range of nT.

Technology developments are needed because advanced solid-state sensors yield measurements in the μT range.

The design, fabrication and characterization of solid-state III-V semiconductor Hall effect sensors are reported in [1-5]. Our objective is to ensure physical and processing compliance, as well as system-centric information fusion and assessment for heterogeneous data. As illustrated in Figure 1, we focus on the following tasks:

Detect → *Process and Identify* [$\mathbf{B}(t,\mathbf{r})$,$\nabla\mathbf{B}$, $f(\Sigma_i\mathbf{B})$] → *Information Fusion* / *Data Retrieval* → *Assess / Manage*.

The key advantages of low-power solid-state sensors are:

- Sufficient accuracy, resolution and bandwidth;
- Exceptional compliance with microelectronics;
- Modularity, usability and scalability;
- Safety and operation in harsh and adverse environments.

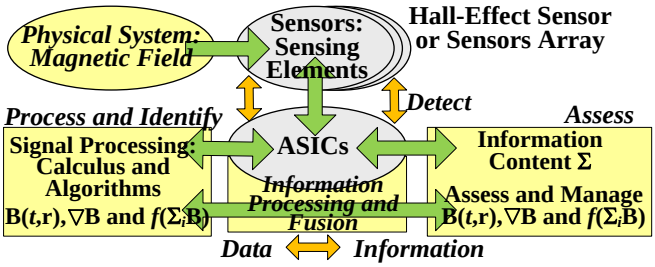

Figure 1. Magnetic field detection, processing and assessment

3. NOISE ANALYSIS

The experimental studies are performed for a Hall effect sensor with a InSb sensing element. There is on-chip compensating circuit and filter. For the normal distribution, the probability density function (pdf) is

$$f_X(x;\mu,\sigma^2)=\frac{1}{\sigma\sqrt{2\pi}}e^{-\frac{(x-\mu)^2}{2\sigma^2}},\ \mu\in\mathbb{R},\ \sigma>0,$$

where the unknown mean μ and standard deviation σ are found by parametrizing pdfs.

The histograms and pdfs are documented in Figures 2 using 800000 samples.The nonlinear least-squares regression yields the unknown μ_i and σ_i which are reported in Table 1.

TABLE 1. Noise in the Sensor–Compensating ICs, and, for the Post-Processed Solution: Parametrized Gaussian Distribution $X_i\sim\mathcal{N}(\mu_i,\sigma_i)$ For Two Data Sets

Magnetic Field B	Gaussian Distribution $X_j\sim\mathcal{N}(\mu_i,\sigma_i)$	
	Integrated Sensor: Sensor–Compensating ICs Output	Post-Processed Filtered Noise
B=0 T	$\mu=1.016\times10^{-7}$, $\sigma=7.289\times10^{-5}$	$\mu=1.967\times10^{-7}$, $\sigma=1.399\times10^{-5}$
	$\mu=-1.864\times10^{-7}$, $\sigma=7.243\times10^{-5}$	$\mu=-3.838\times10^{-7}$, $\sigma=1.418\times10^{-5}$
B=0.3 mT	$\mu=6.188\times10^{-8}$,$\sigma=7.29\times10^{-5}$	$\mu=7.539\times10^{-8}$,$\sigma=1.312\times10^{-5}$
	$\mu=3.308\times10^{-8}$,$\sigma=7.336\times10^{-5}$	$\mu=7.6672\times10^{-8}$,$\sigma=1.401\times10^{-5}$
B=6 mT	$\mu=1.131\times10^{-7}$, $\sigma=7.385\times10^{-5}$	$\mu=8.317\times10^{-7}$, $\sigma=1.505\times10^{-5}$
	$\mu=1.114\times10^{-7}$, $\sigma=7.354\times10^{-5}$	$\mu=-2.716\times10^{-7}$, $\sigma=1.47\times10^{-5}$
B=19 mT	$\mu=8.342\times10^{-7}$, $\sigma=8.412\times10^{-5}$	$\mu=-6.485\times10^{-7}$, $\sigma=1.803\times10^{-5}$
	$\mu=1.001\times10^{-6}$, $\sigma=8.406\times10^{-5}$	$\mu=-7.936\times10^{-7}$, $\sigma=1.785\times10^{-5}$
B=28 mT	$\mu=2.957\times10^{-8}$, $\sigma=8.641\times10^{-5}$	$\mu=-9.031\times10^{-7}$, $\sigma=1.653\times10^{-5}$
	$\mu=1.038\times10^{-7}$, $\sigma=8.701\times10^{-5}$	$\mu=-1.151\times10^{-6}$, $\sigma=1.631\times10^{-5}$

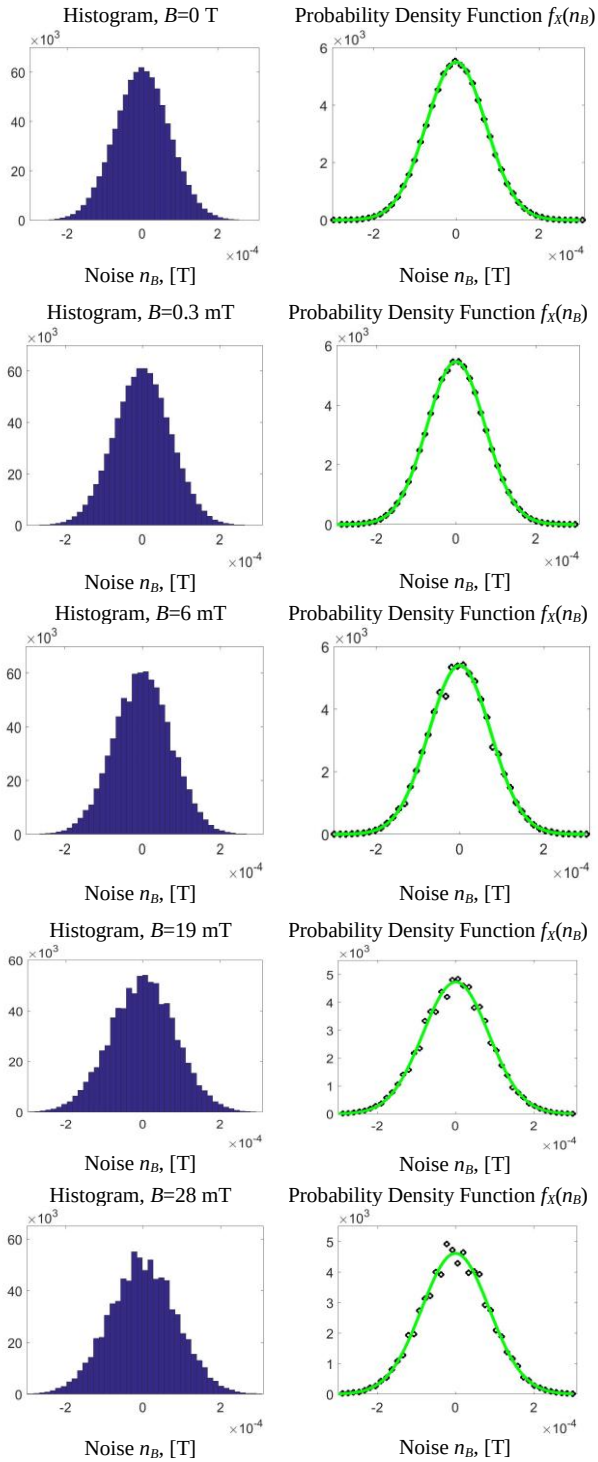

Figure 2. Histograms for the measured sensor noise: Output of the compensating ICs

4. FILTER DESIGN AND SPECTRAL ANALYSIS

We design high-order lowpass Butterworth filters [6-8]

$$H(s)=\frac{k}{B_n(s/\omega_c)},$$

where k is the gain; B_n is the Butterworth polynomial; ω_c is the cutoff frequency.

Depending on dynamic modes, the cut-off frequency ω_c may vary. For ω_c=10000 rad/s, the measured and filtered outputs are illustrated in Figure 3. The filtering ensures the noise attenuation to $n_{B\text{peak-to-peak}}$ ~40 μT. Analysis of power spectral density is performed to support our findings. Figure 3 depicts the power spectral density of the integrated sensor with on-chip ICs, and, post-processed outputs. Noise is attenuated, errors are reduced, and, distortions are minimized. The time- and frequency-domain analyses support the needs for post-processing.

Noise Attenuation, Uniform Field B=7 mT

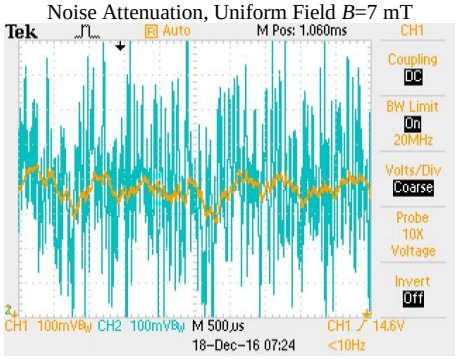

Directly Measured by Sensor,B=7 mT Post-Processed, B=7 mT

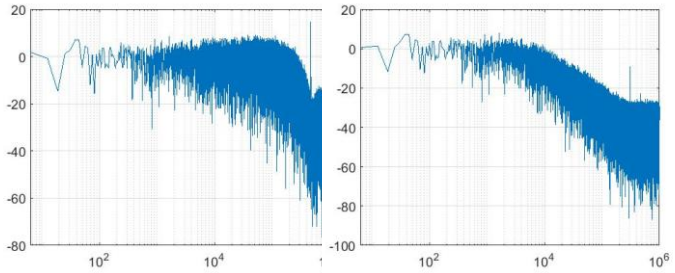

Noise Attenuation, Uniform Field B=16 mT

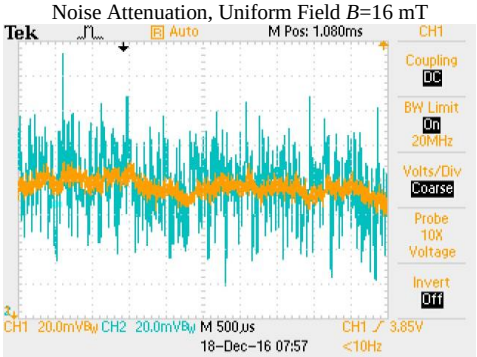

Directly Measured by Sensor,B=16mT Post-Processed, B=16 mT

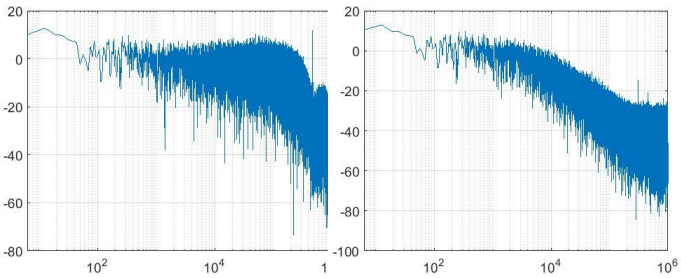

Figure 3. Analysis of multispectral noise $n_B(t)$ and power spectral density for uniform stationary fields (B=const): Measured B by an integrated sensor (Hall effect sensor – compensating ICs), and, with post-processing filter with low power n_B.

The histograms and resulting pdfs are reported in Figure 4. Table 1 documents μ_i and σ_i for the parametrized pdfs assuming the normal distribution. The post-processing allows significantly reduce the standard deviation σ. The statistical analysis indicates accuracy improvements in measuring $B(t,x)$ by using post-processing ICs.

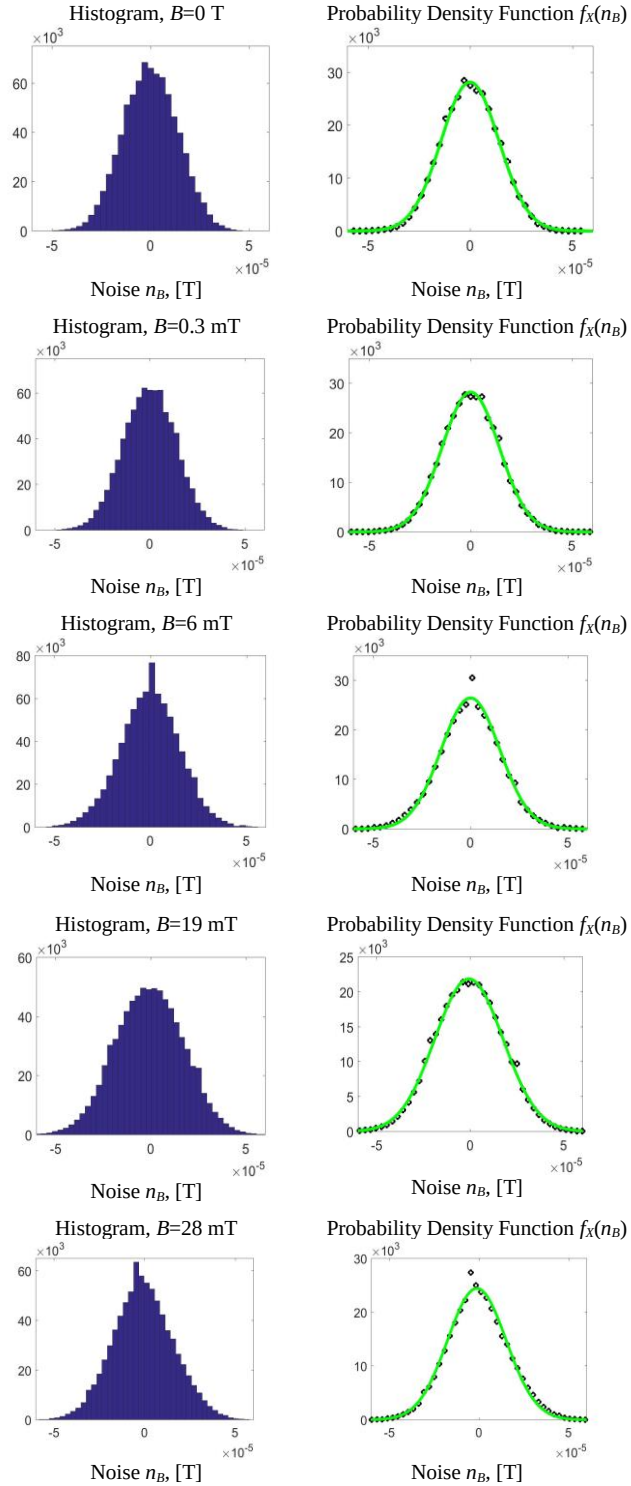

Figure 4. Filtered noise: Histograms and pdfs for $X_j \sim \mathcal{N}(\cdot)$

5. ADAPTIVE SIGNAL PROCESSING

Adaptive signal processing algorithms are designed, implemented and verified. For fast-varying magnetic field $B(t,x)$, Figure 5 documents the directly-measured and post-processed estimates. Hall effect sensors with the proposed post-processing approach improve spatial and temporal resolutions, accuracy, precision, linearity, etc. The proposed solution ensures ~50 μT resolution in measuring fast-varying spatiotemporal magnetic fields with less than 300 μsec latency. The developed concept can be applied and effectively used for other Hall effect sensors.

Applications – Experimental studies indicate that overall objectives and goals are achieved. The proposed technology can be used in various dynamics systems [11-18] and CPS.

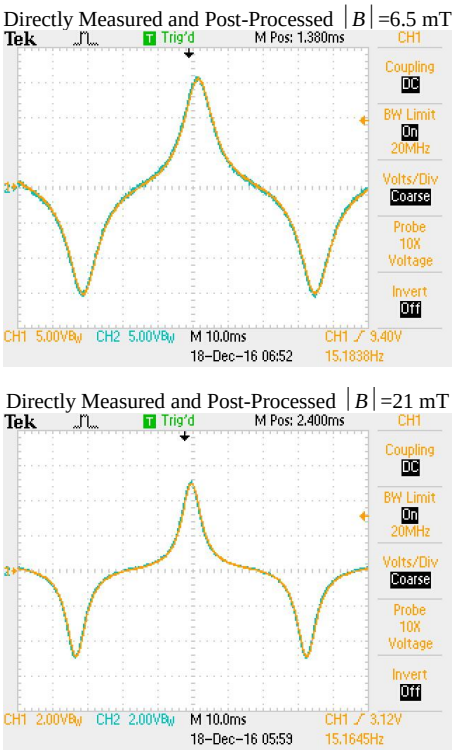

Figure 5. Measured and processed spatiotemporal magnetic field $B(t,x)$ which varies at frequency f=15.2 Hz

6. CONCLUSIONS

Noise attenuation and error reduction problems were researched and solved. High-fidelity data analysis, adaptive filtering and estimation were accomplished for $B(t,r)$, ∇B and $f(\Sigma_i B)$ by using adaptive signal processing. The results were experimentally verified. Performance and capabilities of III-V Hall effect sensors were examined. Hardware, algorithmic and software solutions were proposed and justified to enable measurement, processing, fusion and acquisition capabilities. The use of advanced hardware and proven solutions enable transfer of our findings to high-fidelity operational environment in various applications for diverse platforms. The key components and algorithm validations in laboratory environment were achieved.

REFERENCES

[1] R. S. Popovic, *Hall Effect Devices*, CRC Press, Boca Raton, FL, 2003.

[2] E. Ramsden, *Hall Effect Sensors: Theory and Applications*, Elsevier, Amsterdam, 2006.

[3] Y. Amemiya, H. Terao and Y. Sakai, "Electrical properties of InSb based mixed crystal films," *J. Appl. Phys*., vol. 44, pp. 1625-1630, 1973.

[4] J. Heremans, "Solid state magnetic field sensors and applications," *J. Phys. D: Appl. Phys*., vol. 26, pp. 1149-1168, 1993.

[5] G. S. Lee, P. E. Thompson, J. L. Davis, J. P. Omaggio and W. A. Schmidt, "Characterization of molecular beam epitaxially grown InSb layers and diode structures," *Solid State Electron*., vol. 36, pp. 387-389, 1993.

[6] S. E. Lyshevski, *MEMS and NEMS: Systems, Devices and Structures*, CRC Press, Boca Raton, FL, 2008.

[7] S. E Lyshevski, *Mechatronics and Control of Electromechanical Systems*, CRC Press, Boca Raton, FL, 2017.

[8] S. A. Pactitis, *Active Filters: Theory and Design*, CRC Press, Boca Raton, FL, 2007.

[9] P. C. Krause and O. Wasynczuk, *Electromechanical Motion Devices*, McGraw-Hill, New York, 1989.

[10] P. C. Krause, O. Wasynczuk, S. D. Sudhoff and S. Pekarek, *Analysis of Electric Machinery*, Wiley-IEEE Press, New York, 2013.

[11] S. E. Lyshevski, "Control of high performance induction motors: Theory and practice," *J. Energy Conversion and Management*, vol. 42, pp. 877-898, 2001.

[12] S. E. Lyshevski, "Diesel-electric drivetrains for hybrid-electric vehicles: new challenging problems in multivariable analysis and control," *Proc. IEEE Int. Conf. Control Applications*, pp. 840-845, 1999.

[13] S. E. Lyshevski, *Electromechanical Systems and Devices*, CRC Press, Boca Raton, FL, 2008.

[14] S. E. Lyshevski, "Micro-electromechanical systems (MEMS): motion control of micro-actuators," *Proc. IEEE Conf. Decision and Control*, pp. 4334-4335, 1998.

[15] V. Pappano, S. E. Lyshevski and B. Friendland, "Identification of induction motor parameters," *Proc. IEEE Conf. Decision and Control*, pp. 989-994, 1998.

[16] S. D. Senturia, *Microsystem Design*, Kluwer, Norwell, MA, 2001.